Benchmarking inversion methods over the Agat play using reimaged data over the Måløy Slope

Diego Lopez[1]*, Marit Stokke Bauck[1] and Andy Holman[1] compare Extended Elastic Impedance coloured inversion (EEI-CI) and Deterministic Elastic Impedance (DEI) as prospect-scale screening tools for the Agat play on the Måløy Slope in the Norwegian North Sea.

Abstract

Recent success in exploring the Lower Cretaceous Agat play in the Norwegian North Sea can partly be attributed to improved seismic imaging and integrated subsurface evaluation work conducted on the Northern Viking Graben dataset. The play targets deep marine reservoir sands, fed from an exposed source area in the east (Hansen et al., 2021). Seismic attribute maps are useful for identifying the sediment fairways and sand accumulations (Pene et al., 2024); however, identifying hydrocarbon-filled sands remains challenging. Viridien has conducted a test of inversion techniques to evaluate which methods prove useful over large areas of interest. Both Extended Elastic Impedance coloured inversion (EEI-CI) and Deterministic Elastic Inversion (DEI) were evaluated as exploration screening tools for the Lower Cretaceous Agat play on the Måløy Slope, offshore Norway. The study covers 600 km² using 3D seismic angle stacks and a limited set of wells with elastic logs. While EEI-CI provides rapid reconnaissance of the major fairways, it exhibits reduced spatial continuity and local false positives. DEI better resolves sand-body architecture and fluid fill, including correct discrimination of known dry wells, and remains robust when well-control configuration is reduced.

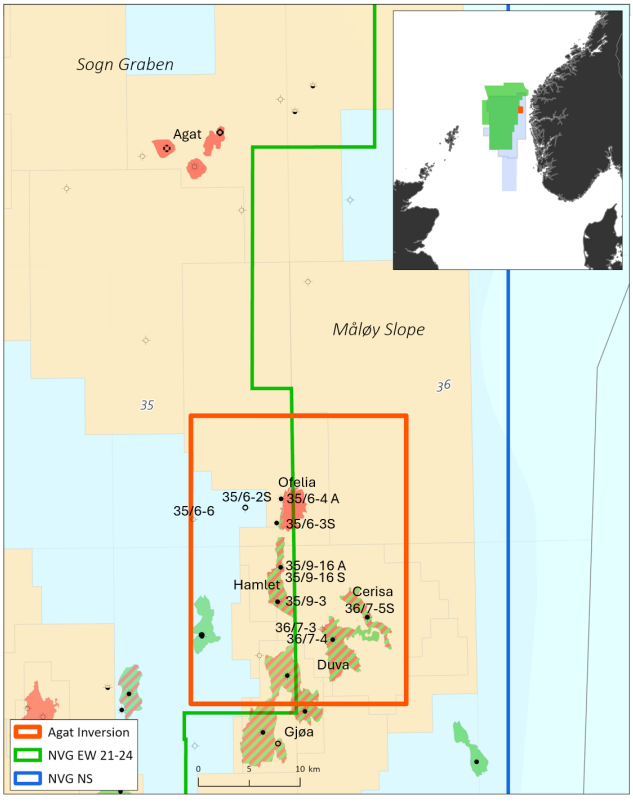

Figure 1 Location map of the study area (orange polygon) off the coast of Norway. The reimaged NVG (CGG23M04) dataset covers the full area (blue polygon), while an additional EW dataset covers the western part (green polygon).

Introduction

The Lower Cretaceous Agat Formation of the Northern North Sea contains sandstone reservoirs deposited from deep-water turbidite flows. These are commonly represented in seismic data as channelised to fan-like geometries within both open-slope and confined-basin environments. The Agat play was proven by wells in block 35/3 in the nineties (Skibeli et al., 1995). In this study, we investigate the more recent success in blocks 35/6, 35/9 and 36/7 (Figures 1 & 2). Here, the reservoir thickness is typically ~10 m of sand and conglomerate units, or more heterogeneous units of a total of 200 m with several thinner sand intervals. Porosity is up to 25-28% (Hansen et al., 2021). The Agat sand reservoirs host a producing field (Duva) and several discoveries (e.g., Hamlet, Ofelia, and Cerisa, Figures 1 & 2). However, reservoir heterogeneity, sand distribution and quality vary, leading to differences in seismic amplitude response. Challenges in predicting mixed lithology and pore-fluid fill have led to some unsuccessful wells.

From an exploration standpoint, the main uncertainties are (i) defining sand-body architecture, including feeder systems, connectivity and seals, and (ii) predicting fluid distribution, including distinguishing between hydrocarbon-bearing and brine-filled zones. These uncertainties are especially significant where well control is limited or unevenly distributed, and where rapid decisions must be made across large areas using seismic data with limited calibration.

Seismic inversion methods used in exploration range from quick, attribute-based screening to more detailed, model-driven inversion. EEI-CI provides a fast reconnaissance option by converting AVO intercept and gradient data into rotated impedances

[1] Viridien
* Corresponding author, E-mail: diego.lopez@viridiengroup.com
DOI: 10.3997/1365-2397.fb2026040

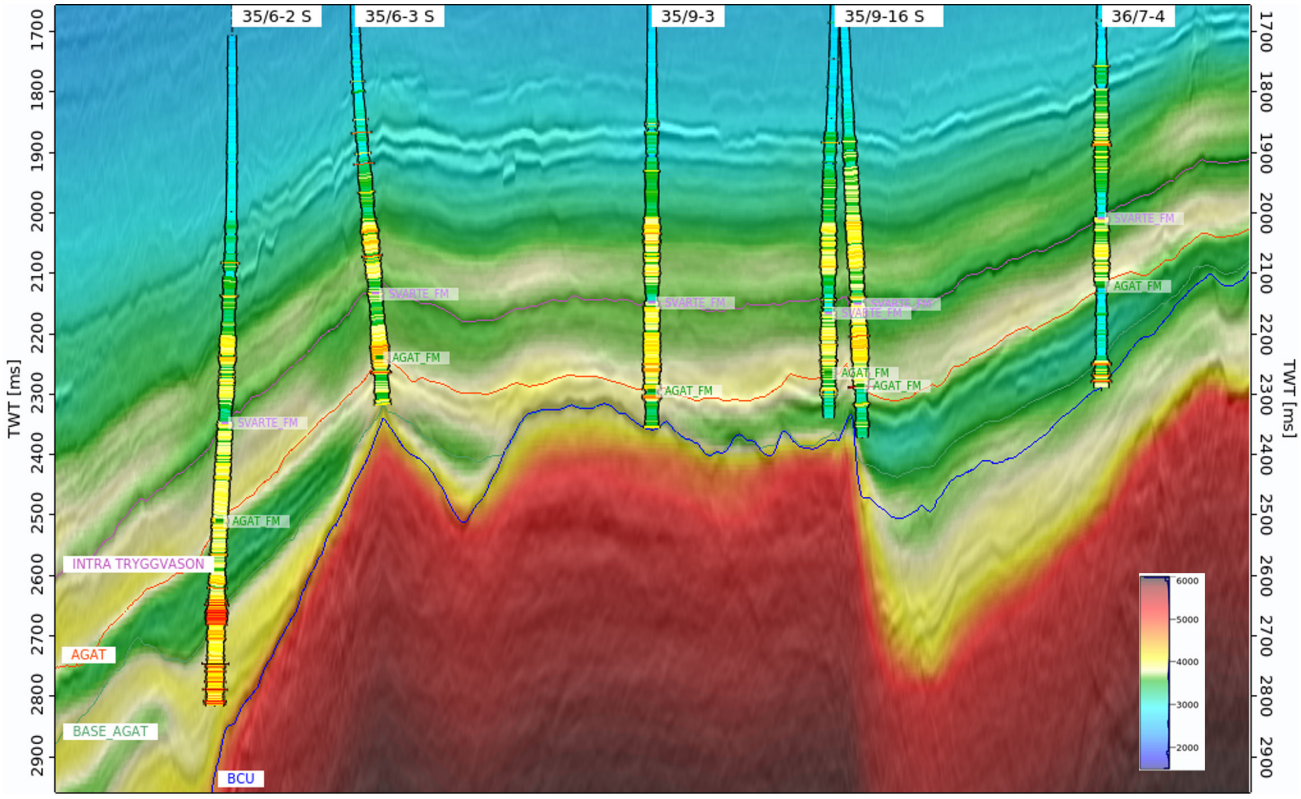

Figure 2 Seismic section overlain with imaging velocities, interpreted horizons and wells with Vp well logs. Wells shown are 35/6-2 S, 35/9-3 Hamlet, 35/9-16A, S Hamlet appraisal and 36/7-4 Duva. Velocity data is from 1500 (blue) to 6000 m/s (red). The blue horizon is the BCU, and the orange horizon is the Top Agat Formation. The high velocities (red) reflect dense Caledonian lithologies such as schists and gneiss.

that relate to lithology and fluid-sensitive properties (Whitcombe et al., 2002). EEI-CI workflows typically require minimal prior modelling and can be applied quickly across large survey areas. However, EEI-CI attributes are naturally band-limited and sensitive to the quality and consistency of the angle stacks used to calculate intercept and gradient. Interpretation can be impacted by noise and residual AVO artifacts. Additionally, EEI-CI attributes depend on consistent behaviour to translate the effects into a single χ angle.

DEI aims to estimate elastic properties (Vp, Vs and density) that best explain observed angle-dependent amplitudes, using wavelet information and a low-frequency initial model. When implemented in a stratigraphic grid and constrained laterally, DEI can yield stable, laterally coherent elastic volumes from which lithology and fluid probabilities can be derived using Bayesian classification or rock-physics transforms. While DEI typically requires more inputs and QC steps than EEI-CI screening, it can reduce interpretation ambiguity and better support prospect risk assessment. This is particularly relevant in areas where reservoir units are thin and facies variability is pronounced.

This article compares EEI-CI and DEI as prospect-scale screening tools for the Agat play on the Måløy Slope. An overview of the data preparations for these methods is outlined in Figure 3. In the following, we first document the seismic conditioning required to stabilise AVO and inversion, then we present the resulting lithology and fluid products. Finally, we quantify well-based performance using log-to-inversion correlations. We also evaluate sensitivity to reduced well control through a simplified ('minimal-well') inversion configuration and provide practical guidance for selecting an appropriate workflow.

Seismic dataset

The study area covers 600 km² across the Hamlet and Ofelia discoveries and the Duva Field in the North Sea, offshore Norway (Figure 1). The main dataset used is part of the CGG23M04, which is a 3D seismic reimaging of the NVG (CGGM18) dataset, first processed in 2016. The survey was acquired using a N-S-oriented towed-streamer configuration and provided in the two-way-travel time (TWT) domain. Angle-stack ranges are 5-15° for near, 13-23° for mid, 21-31° for far, 29-39° for ultra-far, and 4-32° for full stack. The bin size is 12.5 × 12.5 m, with a 4 ms sampling interval and a 9000 ms record length. A seismic migration velocity field derived from Full-Waveform Inversion (FWI) up to 15 Hz, followed by multi-layer tomography, was used for depth-to-time conversion to support low-frequency modelling (Figure 2).

The interpreted horizons define major stratigraphic units, converted from depth to time using the vertical component of the migration velocity field (Figure 2). Key horizons included the Intra-Kyrre Formation, Intra-Tryggvason Formation, Top Agat Formation, Base Agat Formation, Base Cretaceous Unconformity (BCU) and Top Basement. The Agat interval (Top Agat to Base Agat) was the primary target for lithology and fluid analysis.

Multiple wells intersect the survey area; six wells have a full suite of elastic logs (Vp, Vs, density) and supporting petrophysical logs. Petrophysical QC was performed to check log integrity,

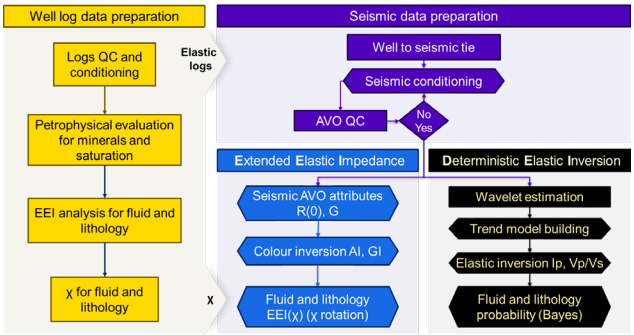

Figure 3 Overview of the well data preparations and EEI-CI and DEI workflows evaluated in this study.

with minor patching and editing where required. One well (35/6-3S) exhibited inconsistent elastic-log behaviour that could not be corrected reliably and was excluded from the study.

Petrophysical properties were standardised across wells. For lithology, the volume of shale (Vsh) was computed using neutron-density logs, effective porosity from a deterministic mineral model (N–D–Separation), and water saturation (Sw) using Archie parameters a=1, m=2, n=2. The crossplots of the elastic properties, where lithology is coloured by facies in Figure 4, illustrate the overlap of each facies in the elastic domains. These logs were used for EEI-CI χ-angle optimisation and for training lithology/fluid probability functions.

AVO sensitivity tests showed that residual angle-dependent spectral differences and minor misalignment across stacks could bias intercept/gradient and downstream attributes. Global angle-based spectral balancing and trim statics were applied. This improved well ties and stabilised gradient behaviour. Radon de-multiple tests reduced coherent noise, but tended to dim anomalies and were not carried forward.

Wavelet estimation was conducted after conditioning. Statistical wavelets were derived from seismic data within a window covering the Intra Kyrre Formation to Base Agat Formation. Deterministic wavelets were extracted per well and averaged to create multi-well wavelets. Phase scanning revealed a tightly clustered distribution near zero phase (averaging around +4°), supporting the use of constant (near-zero) phase wavelet options in specific inversion tests and streamlined workflows. Generally, deterministic wavelets improved the seismic-to-synthetic match, but statistical wavelets enabled a 'minimal-well' inversion workflow, which is useful in sparse-calibration scenarios.

Low-frequency modelling was approached using depth-of-burial trends derived from well logs, including separate shale and sand trends for Vp and empirical transforms for Vs and density. For this study, we deliberately chose to use a less constrained approach, opting to use a depth of burial trend instead of the calibrated velocity from the 15Hz FWI. Stratigraphic inversion was conducted in a grid defined by interpreted horizons above and below the Agat Formation. Micro-layer thickness tested down to ~6 ms without instability. Alternative initial models (machine-learning Vp volume; shale-only trend) were tested to evaluate sensitivity and to support minimal-well inversion scenarios.

EEI coloured inversion

EEI-CI screening was based on the AVO intercept (R0) and gradient (G) derived from a three-term Shuey approximation. Furthermore, the intercept and gradient were converted into relative impedance attributes through coloured inversion. The coloured inversion operator combines a phase rotation with a shaping filter that matches the impedance spectrum derived from well data to the seismic bandwidth, yielding:

Acoustic Impedance (AI) from coloured inversion of the intercept (equivalent to EEI-CI at χ=0°)

Gradient Impedance (GI) from coloured inversion of the gradient (equivalent to EEI-CI at χ=90°)

EEI-CI volumes were generated by combining AI and GI through a χ-rotation in the EEI space (Figure 5). Well-log crossplots of AI versus GI, coloured by saturation and lithology

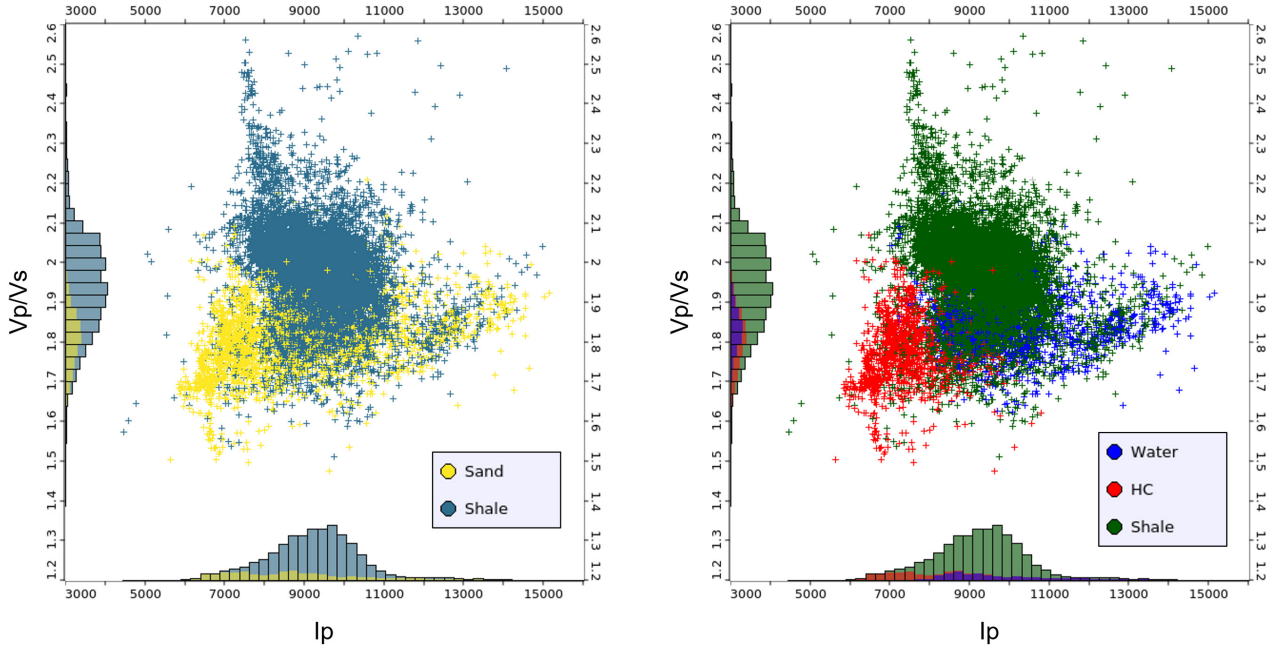

Figure 4 P-Impedance and Vp/Vs crossplots showing classification of lithology (left) and fluid (right).

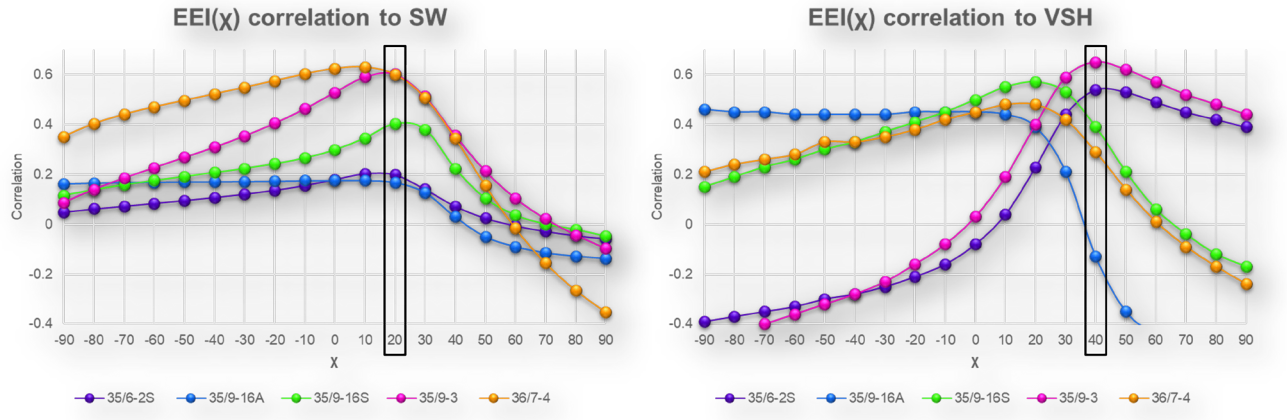

Figure 5 χ rotation analysis for fluid (left) and lithology (right). The ambiguity in the optimum value of chi for the lithology can be observed.

indicators, were used to select χ (Chi) values that maximise separation between classes. A correlation scan over χ demonstrated an average optimum near χ≈20° for fluid effects (low EEI-20 corresponding to hydrocarbons relative to brine) and χ≈40° for lithology (low EEI-40 corresponding to sand relative to shale). The lithology scan was often ambiguous, indicating that a single χ was insufficient to map sand channels consistently, as brine-bearing sands overlapped the shale response due to sand heterogeneity (Figure 4). EEI-CI volumes were then interpreted using interval extractions across Top Agat–Base Agat and along arbitrary sections tied to wells.

EEI-CI is attractive for early-stage screening because it is fast, requires limited a priori modelling, and produces intuitive reconnaissance attributes that often track fairway-scale sand and fluid anomalies. Limitations observed here include higher apparent noise levels, reduced spatial continuity, and local over-optimism in fluid prediction (false positives) where lithology/fluid trends overlap in the AI-GI space or where residual AVO artefacts persist.

Deterministic Elastic Inversion

DEI was implemented as a multi-trace, stratigraphic-grid simultaneous inversion that estimates Vp, Vs and density, and updates stratigraphic layer thickness (TWT) to optimise the match between modelled angle-dependent responses and the input angle stacks through a simulated-annealing-based iterative method

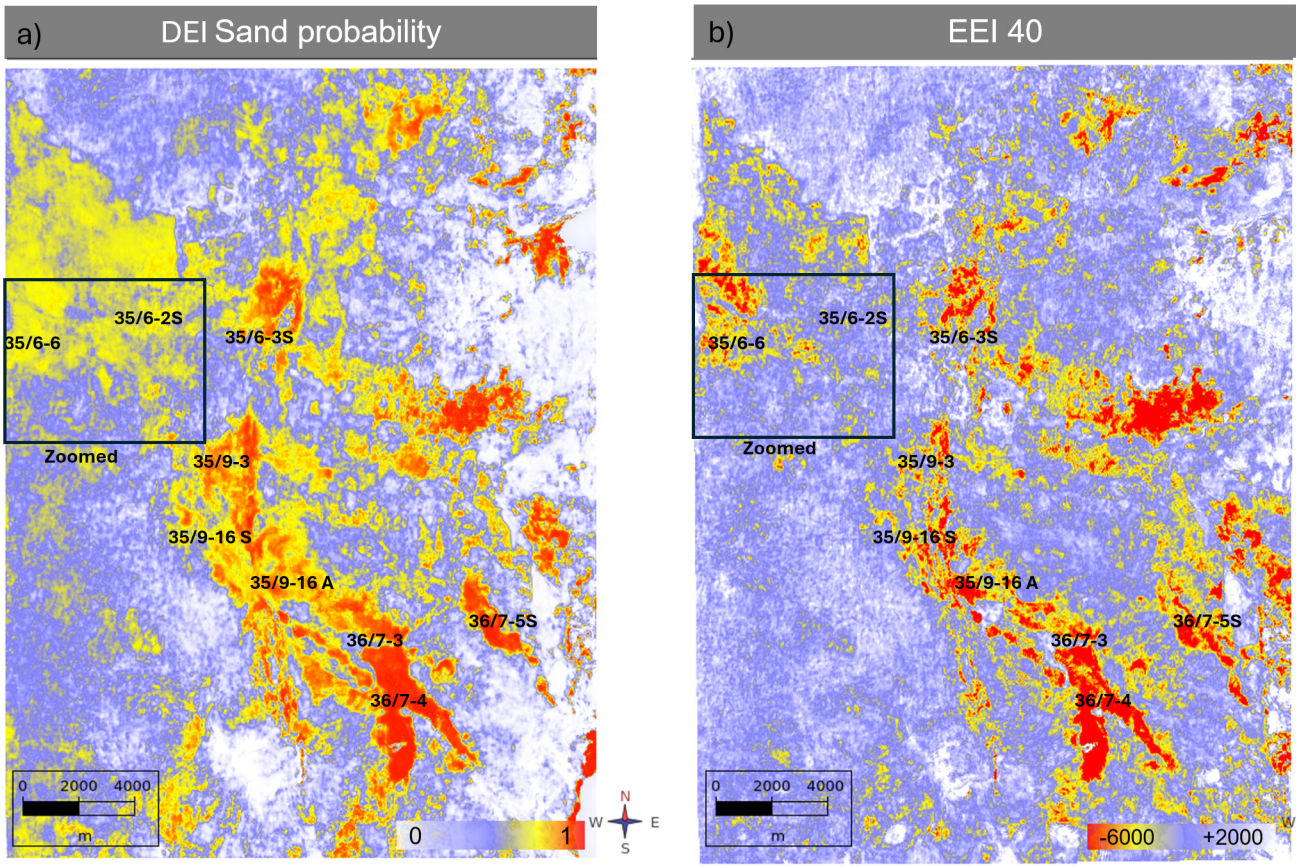

Figure 6 Horizon slice of a) DEI sand probability and b) EEI40 lithology. The black polygon indicates the zoomed area in Figure 10.

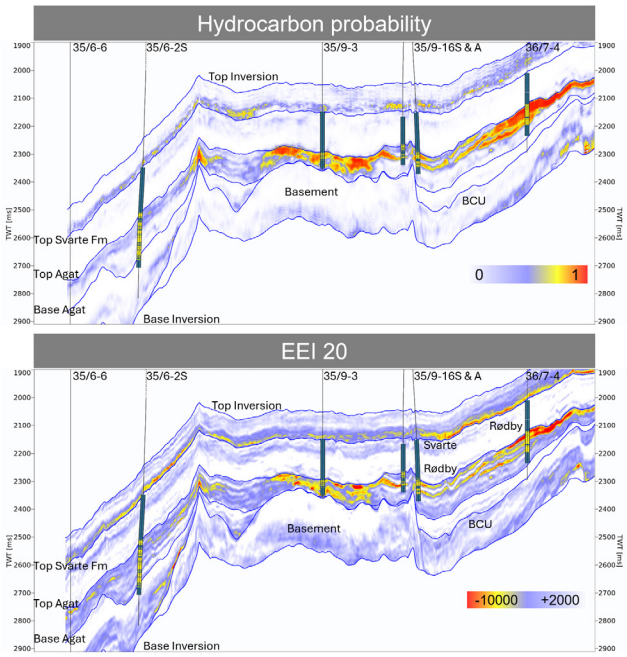

Figure 7 Hydrocarbon probability from DEI (shale trend) and EEI20, which represents fluid. Well data colours indicate shale (blue) and sand (yellow).

(Coulon et al., 2006). The DEI operates on 3D neighbourhoods to enforce lateral continuity.

Wells were tied to the full stack using checkshots where available, with mild stretch/squeeze calibration. Wavelets were estimated using both statistical and deterministic well-based extraction methods. Inversion tests included mixed-phase and constant/zero-phase wavelets; constant/zero-phase wavelets improved the definition of some Vp/Vs responses in the target interval.

Horizons were used to define macro units within which micro-layering was constructed. Layer thickness sensitivity tests were performed, decreasing from 10 ms to 6 ms. A minimum micro-layer thickness of ~6 ms improved vertical resolution without introducing visible instability.

The typical approach for building initial models is to interpolate well logs and use the seismic imaging velocity field as an external trend. However, here we used depth-of-burial trends derived from well logs, with separate sand and shale trends for Vp, and empirical relationships for Vs and density. This represents a deliberately simplified, non-conventional LFM (low-frequency initial model) strategy, chosen to keep the inversion as unconstrained as possible. This provides a plausible low-frequency background beyond the seismic band limit and better captures compaction-related trends that influence facies discrimination.

Lithology and hydrocarbon probability volumes were generated using Bayesian classification trained on well-log-derived facies definitions (Hampson et al., 2010). Sand and shale facies were defined using a Vsh cutoff of 0.4. Classification was tested in multiple elastic domains; for lithology and fluid prediction, P-impedance versus Vp/Vs ratio provided the most robust behaviour for key wells and areas of limited calibration. Fluid prediction used litho-fluid classes based on Vsh and saturation, producing hydrocarbon probability volumes (gas + oil) and water/shale probabilities (Figure 4).

EEI-CI products

EEI-20 and EEI-40 interval extractions across the Agat interval delineate a coherent fairway consistent with a channelised turbidite system, and anomalies coincide with known discoveries in the area (Figures 6 & 7). The EEI-CI approach provides rapid reconnaissance and is effective for identifying the main channel trend and several prospective anomalies, although the response at the latest discovery (36/7-5S Cerisa) is not especially diagnostic of a well-delimited channel-body anomaly (Figure 6b). More generally, EEI-CI attributes show reduced spatial continuity and strong sensitivity to display scaling, and local misclassification occurs where lithology and fluid effects overlap in the EEI space. A limitation observed is a false-positive hydrocarbon indication at a known dry well: at 35/6-6, EEI-20 indicates a hydrocarbon-like response despite brine fill (Figures 6 & 7). Logs are not available for this well.

DEI products

DEI produces laterally coherent elastic volumes (Vp/Vs, impedance and density). Inversion-derived sand probability maps delineate connected sand bodies through the Agat interval and better resolve continuity and geometry than EEI-40 screening, particularly in areas where EEI-CI attributes appear noisy or disconnected (Figure 7).

Hydrocarbon probability derived from Bayesian classification shows strong agreement with known discoveries and is in alignment with dry wells (35/6-2S and 36/7-3 in Figure 7). At 35/6-6, where EEI-20 suggests hydrocarbons, the DEI-derived hydrocarbon probability is very low (<10%), indicating robust suppression.

Well-log validation confirms high agreement between inverted and measured elastic properties. In the DEI, the sand/

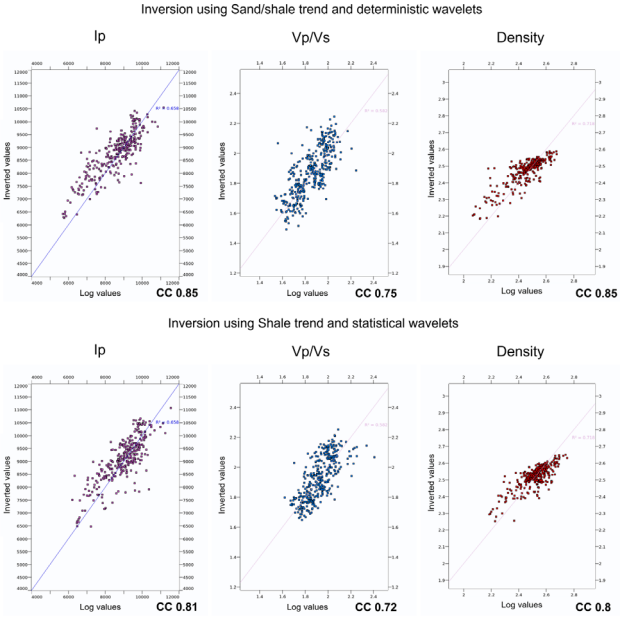

Figure 8 Well log vs inversion correlation for inversion using sand/shale trend + deterministic wavelets (upper part) and shale trend + statistical wavelets (lower part). X axis: log, Y axis: inverted, P-impedance (g/cm3, m/s), Vp/Vs (dimensionless), density (g/cm3).

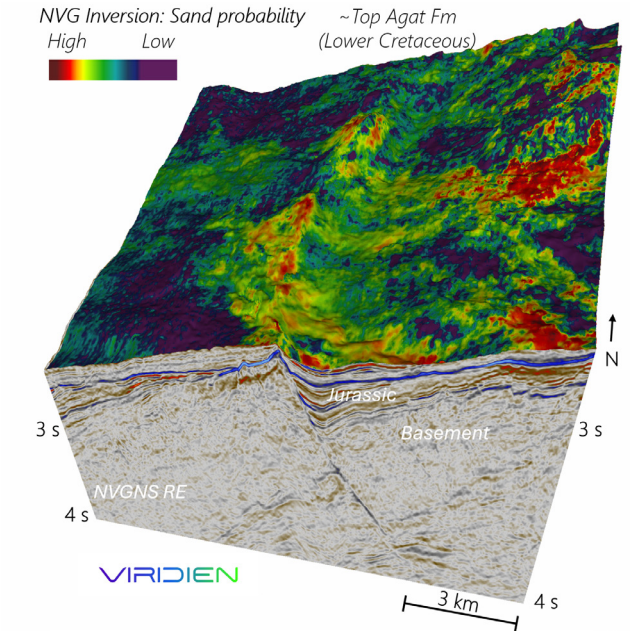

Figure 9 Sand probability from Deterministic Elastic Inversion, viewed from the south. The seismic cube is sliced across the known discoveries.

shale trend initial models and deterministic wavelets achieved correlation coefficients (CC) of 0.85 for P-impedance, 0.75 for Vp/Vs, and 0.85 for density (upper part of Figure 8). A reduced well-control variant using statistical wavelets preserved a similar performance of 0.81 for P-impedance, 0.72 for Vp/Vs, and 0.8 for density, supporting use in sparse-calibration settings (lower part of Figure 8).

The minimal-well inversion configuration (statistical wavelets and simplified trend modelling) remains only slightly degraded relative to the constrained case while retaining the advantages of inversion-derived probability products. This provides a practical route for extending the workflow into areas with limited well control without reverting to purely qualitative screening attributes.

Discussion

EEI-CI is most effective as a rapid reconnaissance workflow for large areas and early-stage ranking. It requires limited modelling and can be used to map first-order fairways and identify candidate anomalies for follow-up work. In this study, EEI-CI successfully highlights the principal Agat fairway and several known accumulations (Figure 6b).

DEI is preferable when reliable discrimination of sand architecture and fluid limits is required, or when false positives have material decision impact. In this dataset, inversion-derived Bayesian hydrocarbon probability suppresses an EEI-CI false positive at 35/6-6 and provides more coherent, geologically plausible sand-body geometry than EEI-40 screening. The preferred inversion result is shown in Figure 9 on a sculpted seismic cube.

A practical exploration workflow is to apply EEI-CI first to identify fairways and prioritise targets, then deploy DEI selectively over ranked areas to refine geometry and reduce ambiguity in fluid risk. EEI-CI outputs can also guide inversion parameter selection (e.g., interval windows, expected χ trends), while DEI yields quantitative elastic volumes and probability products.

EEI-CI remains band-limited and sensitive to residual AVO artefacts and angle-dependent bandwidth differences. DEI relies on stable wavelet estimation and low-frequency trend modelling; model choices (e.g., inclusion of basement velocities) can introduce bias through low-pass filtering below seismic bandwidth.

Summary

A comparative evaluation of EEI-CI and DEI over ~600 km² in the Måløy Slope, Norwegian North Sea demonstrates that both workflows can support Agat play screening, but with different strengths. EEI-CI provides rapid, low-complexity reconnaissance and successfully delineates the principal fairway and major anomalies. However, EEI-CI outputs exhibit reduced spatial continuity and can yield false positives when lithology and fluid responses overlap or when residual AVO artefacts persist.

DEI, implemented in a stratigraphic grid and supported by wavelet estimation, low-frequency trend modelling and Bayesian classification, yields laterally coherent elastic volumes and probability products that better resolve sand-body architecture and fluid limits. A key result is suppression of a dry-well false positive: at well 35/6-6, EEI-20 suggests hydrocarbons, whereas inversion-derived Bayesian classification predicts <10% hydrocarbon probability, consistent with the known outcome (Figure 10). Well-based validation shows strong elastic property agreement for the P-impedance, Vp/Vs, and density correlations for the most constrained configuration. Only slightly reduced values for a minimal-well configuration were observed.

Overall, EEI-CI is recommended for rapid survey-scale reconnaissance, while DEI is recommended when quantitative discrimination of sand geometry and fluid risk is needed.

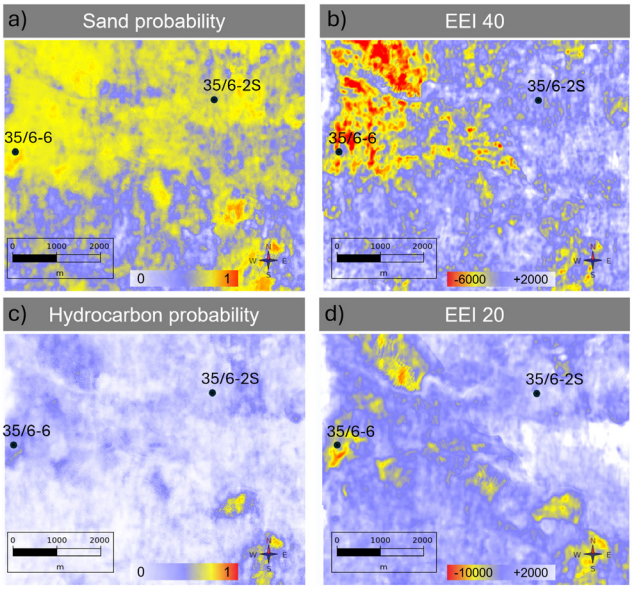

Figure 10 Zoomed maps of the a) DEI sand probability and b) EEI 40 lithology, both shown in Figure 7. The DEI hydrocarbon probability is shown, and in d) the EEI 20 (fluid factor) is shown. The 35/6-6 is known as a dry well, but the EEI-CI results indicate hydrocarbons. This is therefore a false positive, and the result of the DEI is preferred.

Importantly, a reduced well-control inversion variant retains much of the inversion benefit and provides a scalable route to applying quantitative inversion in sparse-calibration exploration settings.

Acknowledgements

The authors would like to thank Viridien's Earth Data business line and Seismic Reservoir Characterisation team for support and permission to publish this comparison.

References

Connolly, P. [1999]. Elastic impedance. *The Leading Edge*, **18**(4), 438-452. Doi: 10.1190/1.1438307

Coulon, J.P., Lafet, Y., Deschizeaux, B., Doyen, P.M. and Duboz, P. [2006]. Stratigraphic elastic inversion for seismic lithology discrimination in a turbiditic reservoir. Doi: 10.1190/1.2369949

Hampson, D. [2010]. Lithology Prediction using Seismic Inversion Attributes. Hampson-Russell, a CGGVeritas Company, 1A62.

Hansen, H.N., Løvstad, K., Lageat, G., Clerk, S. and Jahren, J. [2021]. Chlorite coating patterns and reservoir quality in deep marine depositional systems – Example from the Cretaceous Agat Formation, Northern North Sea, Norway. *Basin Research*, **33**(5), 2725-2744. Doi: 10.1111/bre.12581

Pene, I., Rogne, S. and Bauck, M.S. [2024]. Mapping of Early Cretaceous Sand Fairways on the Måløy Slope, Norwegian North Sea. 85th EAGE Annual Conference & Exhibition, *Extended Abstracts*. Doi: 10.3997/2214-4609.2024101437

Shuey, R.T. [1985]. A simplification of the Zoeppritz equations. *Geophysics*, **50**(4), 609-614. Doi: 10.1190/1.1441936

Skibeli, M., Barnes, K., Straume, T. and Shanmugam, G. [1995]. A sequence stratigraphic study of Lower Cretaceous deposits in the northernmost North Sea. *Norwegian Petroleum Society Special Publications*, **5**, 389-400. Doi:10.1016/S0928-8937(06)80077-9

Whitcombe, D.N., Connolly, P.A., Reagan, R.L. and Redshaw, T.C. [2002]. Extended elastic impedance for fluid and lithology prediction. *Geophysics*, **67**(1), 63-67. Doi: 10.1190/1.1451337